Bragg Spectroscopy of the Multibranch Bogoliubov Spectrum of Elongated Bose-Einstein Condensates

J. Steinhauer,[1] N. Katz,[1] R. Ozeri,[1] N. Davidson,[1] C. Tozzo,[2] and F. Dalfovo[2,3]

[1]*Department of Physics of Complex Systems, Weizmann Institute of Science, Rehovot 76100, Israel*

[2]*Dipartimento di Matematica e Fisica, Università Cattolica del Sacro Cuore, via Musei 41, Brescia, Italy*

[3]*INFM Unità di Brescia and BEC-INFM, Trento, Italy*

(Received 3 September 2002; published 13 February 2003)

We measure the response of an elongated Bose-Einstein condensate to a two-photon Bragg pulse. If the duration of the pulse is long, the total momentum transferred to the condensate exhibits a nontrivial behavior which reflects the structure of the underlying Bogoliubov spectrum. It is thus possible to perform a spectroscopic analysis in which axial phonons with a different number of radial nodes are resolved. The local density approximation is shown to fail in this regime, while the observed data agree well with the results of simulations based on the numerical solution of the Gross-Pitaevskii equation.

DOI: 10.1103/PhysRevLett.90.060404 PACS numbers: 03.75.Kk, 32.80.Lg, 67.40.Db

The crossover between phonon and single-particle excitations in the Bogoliubov spectrum of a weakly interacting Bose gas [1] is one of the main "textbook" concepts that can be directly tested in the case of trapped Bose-Einstein condensed gases. Bogoliubov quasiparticles have been already produced in elongated condensates by using two-photon Bragg scattering [2–5]. For excitations with frequency ω and wave vector k, the phononic character has been checked by observing that the static structure factor $S(k)$ is less than 1 [2,4], by measuring the quasiparticle amplitudes u_k and v_k [3,6], and by showing that the dispersion relation $\omega(k)$ is linear at low k [4,5].

In all of these cases, the local density approximation (LDA) has been used to adapt the Bogoliubov theory of uniform gases to the actual inhomogeneous condensates. This approach is expected to be accurate for large condensates, where the density profile varies smoothly on the scale of the excitation wavelength and the system behaves locally as a piece of uniform gas with a local Bogoliubov spectrum [7,8]. This applies, for instance, to axial excitations of elongated condensates, when the wavelength of the excited states is much smaller than the size of the system along the major axis. These excitations can then be classified with a continuous wave vector k. However, the finite transverse size of the condensate also produces a discreteness of the spectrum, which is ignored in LDA (see [9] for a recent classification of normal modes in anisotropic condensates and [10,11] for the limiting case of an infinite cylinder).

In this Letter we show that the response of the condensate to a Bragg pulse is indeed significantly affected by the radial degrees of freedom. In particular, if the duration of the pulse is longer than the radial trapping period, the condensate responds resonantly at the frequencies $\omega_{n_r}(k)$ of axial quasiparticles with n_r nodes in the radial direction. By using Bragg pulses longer than in previous measurements [2,4], we resolve this multibranch spectrum, finding good agreement with the predictions of the Gross-Pitaevskii (GP) theory.

As described in Ref. [4], our condensate consists of $N = 10^5$ atoms of ^{87}Rb, with a thermal fraction of 5% or less. The radial and axial trapping frequencies are $\omega_\perp = 2\pi(220\ \text{Hz})$ and $\omega_z = 2\pi(25\ \text{Hz})$, respectively. The radial and axial Thomas-Fermi radii of the condensate are $R = 3.1\ \mu$m and $Z = 27.1\ \mu$m.

We excite the condensate by using two Bragg beams with approximately parallel polarization, separated by an angle θ. The Bragg beams illuminate the entire condensate for a time t_B. The beams have a frequency difference ω determined by two acousto-optic modulators. If a photon is absorbed from the higher-frequency beam and emitted into the other, an excitation is produced with energy $\hbar\omega$ and momentum $\hbar\mathbf{k}$, where $k = 2k_p \sin(\theta/2)$, and k_p is the photon wave number. The wave vector $\mathbf{k}$ is adjusted to be along the z axis. To measure a single point on the excitation spectrum $\omega(k)$, k is fixed by θ, and ω is varied.

The measured quantity is the total momentum transferred to the condensate along z. This is obtained by switching off the trapping potential after the Bragg pulse and taking absorption images of the density distribution of the expanding condensate. In Fig. 1 we show typical results for short Bragg pulses of duration $t_B = 1$ msec. The observed momentum P_z is plotted as a function of ω for three different values of k. In Ref. [4] we made Gaussian fits to these types of curves, taking the position of the maximum to be the quasiparticle dispersion $\omega(k)$ and showing that this dispersion was consistent with the Bogoliubov spectrum in the LDA.

A deeper analysis of the same results can be performed by numerically solving the GP equation for the order parameter of the condensate $\Phi(\mathbf{r}, t)$ [12]:

$$i\hbar\partial_t\Phi = \left(-\frac{\hbar^2\nabla^2}{2m} + V + g|\Phi|^2\right)\Phi, \qquad (1)$$

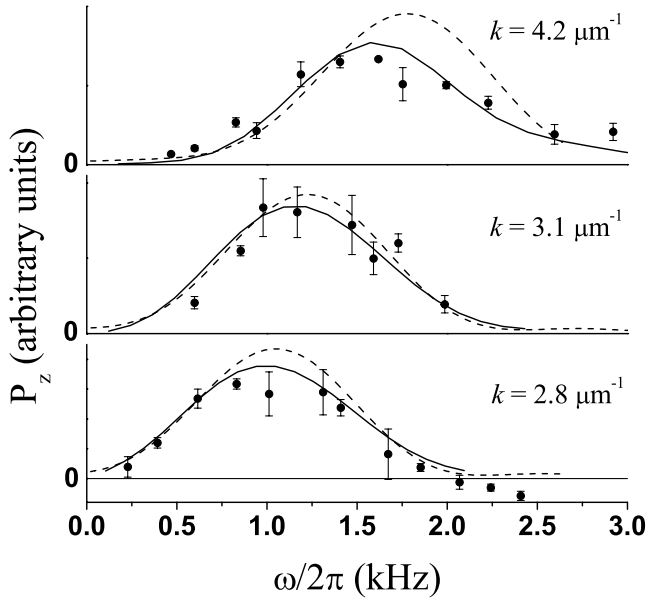

FIG. 1. P_z, in arbitrary units, as a function of ω for short pulses ($t_B = 1$ ms). Bottom, center, and top plots correspond to different k values. Points with error bars are the measured values. Solid lines are the results of GP simulations. The dashed lines are the LDA predictions.

where $g = 4\pi\hbar^2 a/m$ is determined by the s-wave scattering length a. The external potential can be taken as the sum of the harmonic confinement and the Bragg potential,

$$V(\mathbf{r}, t) = \frac{m}{2}(\omega_\perp^2 r_\perp^2 + \omega_z^2 z^2) + \theta(t) V_B \cos(kz - \omega t), \quad (2)$$

where $r_\perp^2 = x^2 + y^2$ and $\theta(t)$ is equal to 1 in the interval $0 < t < t_B$ and 0 outside.

The ground state at $t = 0$ can be found as the stationary solution of Eq. (1). Then, the time dependent GP equation can be solved at $t > 0$ to simulate the Bragg process [8,13]. We take advantage of the axial symmetry of V to map the order parameter into a two-dimensional grid of points $N_\perp \times N_z$ (typically, 64×1024) and evolve it by means of a Crank-Nicholson differencing method with an alternating direction implicit algorithm, as in [14].

The momentum transferred to the condensate can be calculated from Φ through the definition $P_z = (-i\hbar/2) \int d\mathbf{r} \Phi^* \partial_z \Phi + \text{c.c.}$ Figure 1 shows good agreement between the results of the GP simulations (solid lines) and the experimental data, for short pulses. The strength V_B in the GP equation is used as a free parameter, so the comparison is restricted to the position and shape of the peak. In principle, V_B could be determined by using the experimental parameters for the power, area, and direction of polarization of the two laser beams, but this estimate might be affected by a significant uncertainty.

The LDA curves (dashed lines in Fig. 1), which are obtained by using the local Bogoliubov spectrum to calculate $P_z(k, \omega)$ in the linear response regime as in [8], are also reasonably close to the GP predictions. For shorter t_B we checked that the accuracy of the LDA is even better, as discussed in [8].

A rather different situation is found for longer pulses, with t_B on the order of the radial trapping period (about 4.5 msec) [15]. Figure 2 shows the momentum transferred in the GP simulations (solid curves) for various time durations t_B. The lowest curve, after 1 msec, is a broad peak as in Fig. 1, close to the LDA (dashed curves). For longer times however, a multipeak structure appears, strongly deviating from LDA. We find a similar behavior for all values of k in our simulations and for a wide range of intensities V_B.

Figures 3(a) and 3(b) show measurements of P_z for $k = 1.4\ \mu\text{m}^{-1}$ and $3.1\ \mu\text{m}^{-1}$, respectively, with long pulses of duration 10 and 6 msec, respectively. The intensities of the Bragg beams are adjusted so that the number of excitations created on resonance is no more than roughly 25% of the number of atoms in the condensate. Each point in Fig. 3 is an average of about five measurements. The error bars reflect the statistical error of this averaging. The results of GP simulations are indicated by the upper solid curves, which are obtained by choosing $V_B = 0.35\hbar\omega_\perp$ and $0.2\hbar\omega_\perp$ for Figs. 3(a) and 3(b), respectively. Both the measurements and the GP simulations show multiple peaks, due to the excitations of quasiparticles with different n_r.

We verify that the multipeak structure reflects the fundamental normal modes composing the multibranch

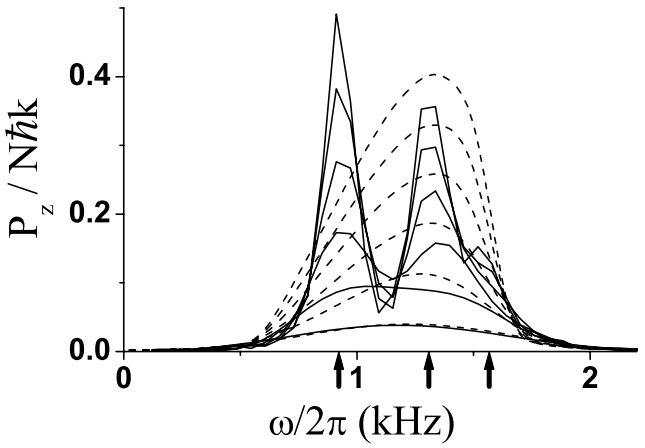

FIG. 2. The time dependence of the momentum transferred during the Bragg pulse, for $k = 3.1\ \mu\text{m}^{-1}$. Solid curves are the results of GP simulations with $V_B = 0.2\hbar\omega_\perp$ plotted at various times. Starting with the lowest solid curve, $t_B = 1, 2, 3, 4, 5,$ and 6 msec. The dashed curves are the corresponding LDA predictions. The arrows indicate the GP predictions for the frequencies of the normal modes of the condensate, having 0, 1, and 2 radial nodes and the same axial wave vector k.

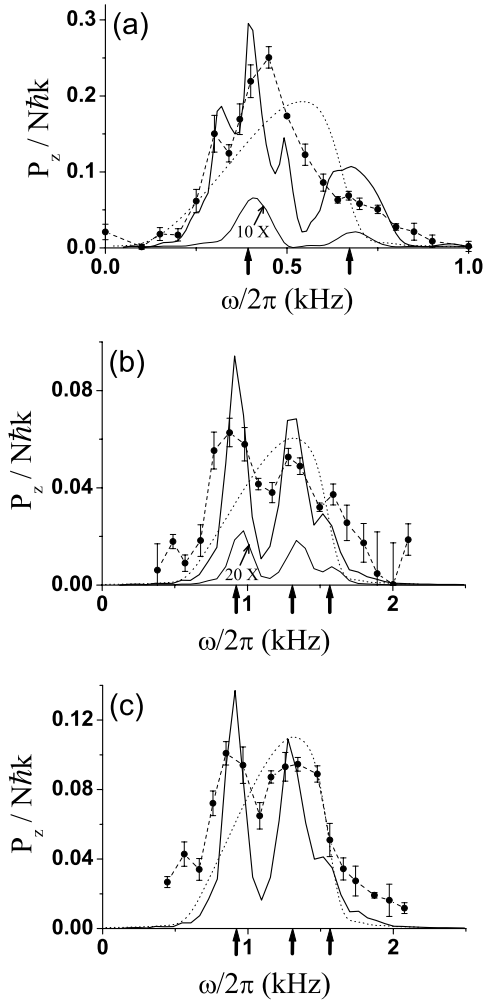

FIG. 3. P_z in units of $N\hbar k$, as a function of ω for long Bragg pulses. For (a) and (b), $t_B = 10$ msec and 6 msec, respectively, and $k = 1.4\ \mu\text{m}^{-1}$ and $3.1\ \mu\text{m}^{-1}$, respectively. The circles are the measured values. The dashed line is a guide to the eye. The upper solid curve is the result of GP simulations with $V_B = 0.35\hbar\omega_\perp$ and $0.2\hbar\omega_\perp$, for (a) and (b), respectively. The lower solid curve is the same but with V_B 10 times smaller. For the lower curve, P_z is multiplied by 10 and 20 for (a) and (b), respectively. The arrows on the ω axes indicate the normal mode frequencies, as in Fig. 2. (c) is the same as (b), but with greater intensity. For the GP simulation in (c), $V_B = 0.26\hbar\omega_\perp$. The dotted curves are the LDA predictions.

spectrum and does not depend significantly on the intensity V_B. The lower curves of Figs. 3(a) and 3(b) correspond to the same simulations as the upper curves, but with V_B reduced by a factor of 10. In this case, the system is excited in the linear response regime. The momentum transferred is 2 orders of magnitude smaller, but the resulting curves have peaks at the same locations as for larger V_B. Furthermore in the case of $k = 3.1\ \mu\text{m}^{-1}$ we repeat the measurement and simulation of Fig. 3(b) with an intensity 30% greater and find peaks again at the same location, as shown in Fig. 3(c). This means that nonlinear effects are not crucial in our observations. Nevertheless, they might be interesting. Indeed, looking at Fig. 3(a) one notices small differences between the lower and upper curves, for small and large V_B, respectively. The curve for large V_B displays two side peaks around the main peak at 0.4 kHz. These side peaks, whose shape significantly depends on t_B, are not visible in the linear regime of the small V_B curve and might be due to nonlinear effects. Similar effects were found by a one-dimensional simulation in Ref. [16].

In Fig. 3, we see good agreement between the locations of the peaks in the experimental and GP results, but the experimental peaks are broader due to noise. The major source of noise is the sloshing of the condensate in the trap. Specifically, sloshing of speed v_{sl} in the axial direction causes a Doppler shift in the light potential of frequency $\Delta\nu_{\text{sl}} = kv_{\text{sl}}/2\pi$. By measuring the velocity of the condensate in the trap at the end of the Bragg pulse from its position in the time-of-flight image, we obtain an estimate for v_{sl}. The corresponding $\Delta\nu_{\text{sl}}$ has a standard deviation of 50, 200, and 150 Hz for Figs. 3(a)–3(c), respectively, which is sufficiently large to account for the observed broadening of the peaks of P_z.

The broadening can be reduced by explicitly adding $\Delta\nu_{\text{sl}}$ for each image to the applied ω in the laboratory frame. This correction requires that the Bragg pulse be much shorter than the axial trap period (40 msec). This requirement is sufficiently met by the 6 msec pulses employed for $k = 3.1\ \mu\text{m}^{-1}$. Therefore, the data points of Fig. 3(b) and 3(c) contain the correction.

A fit of the LDA to the measurements is indicated by a dotted line in Fig. 3. The LDA is seen to fail to reflect the multipeak structure of the measurements.

Now we use the GP equation to directly find the multibranch Bogoliubov spectrum of the condensate. Specifically, we analyze the oscillations in the condensate density induced by the Bragg process. In the GP simulation we let the condensate freely oscillate in the trap after the Bragg pulse and we perform a Fourier analysis of the density variations. This analysis shows that for each k and ω, the density oscillates as a superposition of modes of frequency $\omega_{n_r}(k)$, which are excited by the Bragg potential in Eq. (2) due to the inhomogeneity of the condensate in the radial direction. For symmetry reasons, only modes with azimuthal angular momentum $m = 0$ are excited. The calculated frequencies are shown as open circles in Fig. 4 [17]. The lowest branch corresponds to Bogoliubov axial modes with no radial nodes. The second branch has one radial node; it starts at $2\omega_\perp$ for $k = 0$, where it corresponds to a purely radial breathing mode. The third branch has two nodes [18].

In the limit of small oscillations, all these states coincide with the solutions of the linearized GP equation, i.e., the generalization of the Bogoliubov equations to inhomogeneous condensates. For an infinite cylinder these solutions were calculated in Ref. [10] and, in the

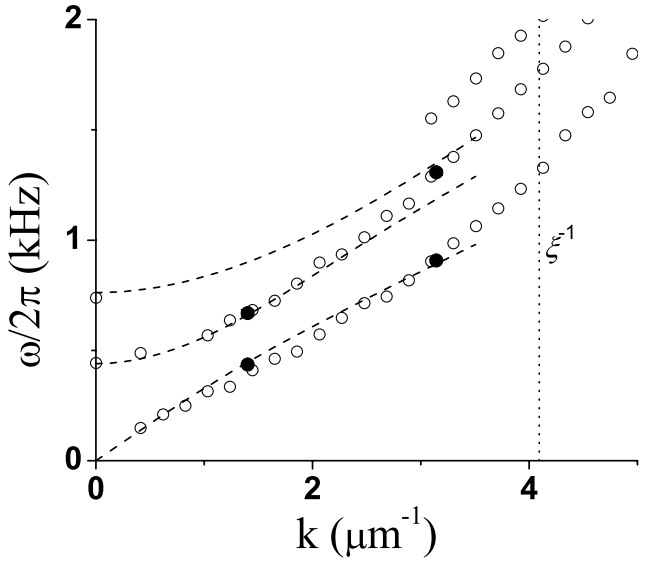

FIG. 4. Excitation frequencies vs k for a trapped Bose-Einstein condensate. The open circles are the frequencies of the normal modes with $n_r = 0, 1, 2, \ldots$ nodes in the radial direction, as calculated from the GP equation. The filled circles are the position of the maxima of the main peaks in P_z for the long-pulse measurements of Fig. 3. The dashed lines are the prediction for an infinite cylinder with $k \ll \xi^{-1}$. The dotted line indicates the inverse healing length.

hydrodynamic limit (k much smaller than the inverse healing length ξ^{-1}), in Ref. [11]. For $k \ll \xi^{-1}$, our multibranch spectrum turns out to be very close to the spectrum predicted in Ref. [11], indicated by dashed lines in Fig. 4 (also see Fig. 1 of Ref. [11]). ξ^{-1} is indicated by a dotted line in Fig. 4.

The calculated normal mode frequencies are shown as arrows on the ω axes in Figs. 2 and 3. Both the theoretical curves and the experimental results clearly show that the momentum is resonantly transferred to the condensate when the Bragg frequency is close to the Bogoliubov branches.

The locations of the measured peaks of Figs. 3(a) and 3(b) are also shown as filled circles in Fig. 4. These locations are found by parabolic fits to the peaks. The good agreement between these measurements and the simulated spectrum (open circles) identifies the peaks in the observed spectrum as being axial quasiparticles with n_r radial nodes. Bragg pulses can indeed be used to perform high-resolution spectroscopy of the multibranch Bogoliubov spectrum of trapped condensates in a regime where the LDA is not applicable.

In conclusion, we have used long Bragg pulses to spectroscopically measure the first and zeroth order radial modes in the phonon spectrum of a Bose-Einstein condensate. These high-resolution measurements agree well with simulations of the Gross-Pitaevskii equation. The local density approximation fails to reproduce these multiple radial modes.

The technique of long Bragg pulses could also be used to resolve inherent dissipation mechanisms, such as inhomogeneous broadening and coupling between modes, including Beliaev and Landau damping. The technique could be particularly effective if the inhomogeneous broadening could be overcome, by means of echo techniques, or the use of nonquadratic optical dipole traps. Finally, very sensitive GP simulations could be used in combination with long pulses, to carefully study nonlinear dynamics.

This work is partially supported by MIUR-COFIN2000 and the Israel Science Foundation.

[1] N. N. Bogoliubov, J. Phys. (Moscow) **11**, 23 (1947).
[2] D. M. Stamper-Kurn *et al.*, Phys. Rev. Lett. **83**, 2876 (1999).
[3] J. M. Vogels *et al.*, Phys. Rev. Lett. **88**, 060402 (2002).
[4] J. Steinhauer *et al.*, Phys. Rev. Lett. **88**, 120407 (2002).
[5] R. Ozeri *et al.*, Phys. Rev. Lett. **88**, 220401 (2002).
[6] A. Brunello *et al.*, Phys. Rev. Lett. **85**, 4422 (2000).
[7] F. Zambelli *et al.*, Phys. Rev. A **61**, 063608 (2000).
[8] A. Brunello *et al.*, Phys. Rev. A **64**, 063614 (2001).
[9] A. A. Penckwitt and R. J. Ballagh, J. Phys. B **34**, 1523 (2001).
[10] P. O. Fedichev and G. V. Shlyapnikov, Phys. Rev. A **63**, 045601 (2001).
[11] E. Zaremba, Phys. Rev. A **57**, 518 (1998).
[12] F. Dalfovo *et al.*, Rev. Mod. Phys. **71**, 463 (1999).
[13] P. B. Blakie and R. J. Ballagh, J. Phys. B **33**, 3961 (2000).
[14] F. Dalfovo and M. Modugno, Phys. Rev. A **61**, 023605 (2000).
[15] A longer time scale is fixed by the axial trapping period (40 ms). For such durations other processes become important (reflection of axial modes at the boundary, center-of-mass motion, nonlinear effects, etc.). This regime is considered in [13].
[16] Y. B. Band and M. Sokuler, cond-mat/0207749.
[17] The calculated frequencies have an uncertainty of the order of 0.05 kHz, due to the finite time interval used for the Fourier analysis.
[18] In this range of k only three branches are visible in the Fourier spectrum. The efficiency of the Bragg perturbation (2) in exciting higher branches increases with k.